



ELSEVIER

Journal of Alloys and Compounds 293–295 (1999) 118–123

Journal of  
ALLOYS  
AND COMPOUNDS

# Neutron diffraction study of the $\text{LaNi}_5\text{-D}$ system during activation

M.P. Pitt<sup>a,\*</sup>, E. MacA. Gray<sup>a</sup>, E.H. Kisi<sup>b</sup>, B.A. Hunter<sup>c</sup><sup>a</sup>*School of Science, Griffith University, Brisbane 4111, Australia*<sup>b</sup>*Department of Mechanical Engineering, University of Newcastle, Newcastle 2308, Australia*<sup>c</sup>*Neutron Scattering Group, Australian Nuclear Science and Technology Organisation, Locked Bag 1, Menai 2234, Australia*

## Abstract

The microstructural changes occurring during the initial absorption of deuterium by virgin  $\text{LaNi}_5$  at  $40^\circ\text{C}$  have been investigated using in-situ neutron powder diffraction. Rietveld profile refinement was used to determine the  $\alpha$  and  $\beta$  phase proportions, lattice parameters and microstrains. In absorption, we found that in the two-phase region (i) the lattice parameters of the  $\alpha$  and  $\beta$  phases were (within resolution) independent of the phase proportions; (ii) the  $\alpha$ -phase diffraction peaks remained essentially unbroadened relative to the virgin metal; (iii) the  $\beta$ -phase peaks were relatively broad with the usual anisotropy of breadth. These findings imply that, as nuclei of  $\beta$  phase form for the first time in a particle that is wholly  $\alpha$  phase, the lattice expansion causes pure  $\beta$  crystallites containing a very high density of lattice defects to fracture off the particle, i.e., decrepitate. Hence the nanoscale mixing and strong mechanical interaction between the  $\alpha$  and  $\beta$  phases noted in multiply cycled material are not observed during the initial absorption of D atoms, because the lattice parameter misfit cannot be accommodated. In desorption, and subsequently, there is sufficient accommodation of the lattice parameter mismatch between the  $\alpha$  and  $\beta$  phases for them to coexist in the same powder particle. © 1999 Elsevier Science S.A. All rights reserved.

*Keywords:* Metal hydrogen; Activation; Neutron diffraction; Strain; Dislocation

## 1. Introduction

Activation is the process by which virgin metal first absorbs hydrogen, typically beginning with the necessary modification of the metal surface. In the case of  $\text{LaNi}_5$ , activation is initiated by simply exposing the metal to a sufficient pressure of hydrogen at around room temperature. A slightly elevated temperature (say  $40^\circ\text{C}$ ) accelerates the process, as does excess hydrogen pressure. While the “activation pressure” depends sharply on the actual alloy stoichiometry, closely stoichiometric material activates readily at  $40^\circ\text{C}$  and about 1 MPa pressure, absorbing to a composition of approximately  $\text{LaNi}_5\text{H}_{6.8}$ . The absorption is attended by decrepitation of the virgin crystals to a fine powder ultimately reaching micron sizes and, after several absorption–desorption cycles, a lowering of the pressure of the absorption isotherm by a factor around 0.8. Diffraction studies [1–3] have shown that severe microstrain is induced by activation and relieved by annealing. Annealing appears to effectively reverse the activation process in that the absorption pressure rises to nearly its initial value [1,4].

The aim of this work was to follow and understand the

evolution of the very distinctive microstructure which characterises the activated metal, revealed in strong anisotropic broadening of the diffraction peaks. This was recently shown [5,6] to be well described by a physical model of scattering by dislocations with density  $>10^{12}\text{ cm}^{-1}$  in the slip system  $(a/3) \langle 2110 \rangle \{0110\}$ , as reported from TEM studies [7].

## 2. Experimental details

The sample was virgin  $\text{LaNi}_{4.93}$  (NUCOR Research Chemicals alloy #1241) of mass 36 g, ground and sieved to sizes between 53 and 106  $\mu\text{m}$ . The sieved powder was quickly transferred to the sample can, and heated and pumped for several hours to remove impurities. The sample remained under vacuum until the experiment commenced. The experiment was conducted at  $40^\circ\text{C}$ . Eleven powder diffraction patterns were recorded during the first absorption and desorption of deuterium using the diffractometer HRPD at the reactor HIFAR operated by the Australian Nuclear Science and Technology Organisation. Data were obtained from  $10^\circ$  to  $154^\circ$  ( $2\theta$ ) in  $0.05^\circ$  steps at  $\lambda=1.8823\text{ \AA}$ . Deuterium was supplied from a metal–deuteride storage reservoir, which also served to purify it.

\*Corresponding author.

The deuterium-to-metal atomic ratio,  $D/M$ , was set using a manometric hydrogenator, by preparing an aliquot of  $D_2$  in a standard reference volume, opening a valve to the sample volume, and measuring the decrease in pressure in the total volume formed. Each change in  $D/M$  was allowed to settle for 1 h before recording a diffraction pattern during absorption, and 1 h during desorption. During absorption, no precautions were taken to avoid compositional inhomogeneity in the sample [8] because the activation pressure is essentially the same for all powder grains. In desorption, small steps ( $\Delta(H/M) \approx 0.05$ ) were taken to minimize the composition spread. The Rietveld profile analysis code LHPM [9] was used to fit the diffraction patterns with a structural model in which the anisotropic line broadening (maximum in  $(hk0)$  directions, minimum in  $(00l)$  directions) is described by a generic basal-plane strain,  $\Delta a/a$ , as previously detailed [2]. This approach is quite satisfactory for the determination of lattice parameters and phase proportions as it exactly emulates the  $(hkl)$ -dependence of the dislocation scattering referred to above. Agreement indices were satisfactory, with  $R_b$  in the range 1–3% for all fits, including two-phase ones.

### 3. Results

Fig. 1 shows the pressure–composition phase diagram derived from the manometric measurements and indicates the values of  $D/M$  at which diffraction patterns were recorded. Fig. 2 shows a two-phase pattern from the central portion of the absorption isotherm, along with the calculated pattern, difference pattern and reflection

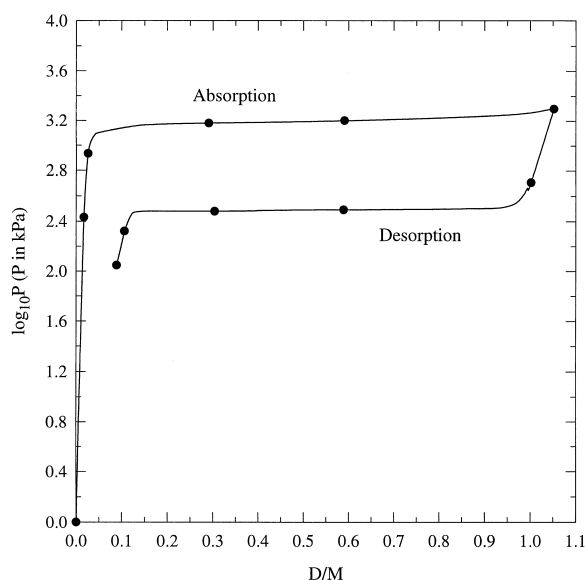


Fig. 1. Pressure–composition phase diagram for the first absorption and desorption of D by  $LaNi_5$  at  $40^\circ C$ . The points indicate where neutron diffraction patterns were recorded. Note that the  $D/M$  scale is derived from pressure measurements. Note also the significant fraction of D not recovered in desorption.

markers. The  $\alpha$  phase was described in space group  $P6/mmm$  and the  $\beta$  phase in  $P31c$  [10]. The sample in this condition was plainly partially activated in the sense that some parts have formed the  $\beta$  phase, with the characteristic anisotropic broadening, while the  $\alpha$ -phase peaks remain close to instrumental in width, albeit shifted to significantly larger d-spacings. Fig. 3 shows a pattern taken at nearly the same  $D/M$  value during desorption. The  $\alpha$  phase observed here has formed from material which underwent the formation of the  $\beta$  phase during absorption, and the anisotropic line broadening is now essentially fully developed in both phases. Fig. 4 summarises the behaviour of the lattice parameters of each phase and Fig. 5 charts the variation of the RMS microstrain as measured by  $\Delta a/a$  [2]. No  $\Delta a/a$  data are shown for the  $\alpha$  phase in absorption because no anisotropy in peak breadth was resolved.

The lever rule was used to express phase proportions (derived from Rietveld scale factors) as Deuterium-to-Metal ratios. The significant amount of D unrecovered in desorption, ie, trapped, presents a dilemma. We chose to regard the trapped D as a third, extraneous phase and rescaled the length of the desorption isotherm accordingly, then read off the concentrations at the phase boundaries and calculated  $D/M$  values from the phase proportions as usual. Figs. 4 and 5 are based on these values.

### 4. Discussion

Fig. 4 reveals the basic mechanism by which the virgin crystallites transform into the cycled fine powder. In common with previous findings [11], in absorption the  $\alpha$  phase expands anisotropically ( $\Delta a \gg \Delta c$ ) to the point of saturation, when the  $\alpha \rightarrow \beta$  transformation begins. Thereafter, the lattice parameters of both phases are constant within the reliability of the refinement, despite the 24% increase of the unit cell volume owing to the  $\alpha \rightarrow \beta$  phase transformation. This means that, as a  $\beta$ -phase nucleus forms in a particle that is initially wholly  $\alpha$  phase, the misfit strain at the  $\alpha$ – $\beta$  interface is rapidly relieved by the  $\beta$ -phase region fracturing and falling away from the parent particle, which is the process of decrepitation. It can be imagined to occur either by internal nucleation of the  $\beta$  phase, leading to splitting of the parent particle, or by surface nucleation, leading to surface spalling. Hence the sample observed at a particular value of  $D/M$  consists mostly of particles which are entirely untransformed ( $\alpha$ ) or fully transformed ( $\beta$ ). It is expected that only a small fraction of the total sample volume will actually be in the process of nucleating the  $\beta$  phase (with elastic accommodation of interfacial strain) and consequently no shift in lattice parameters is visible in the diffraction patterns.

In contrast, the lattice parameters in desorption are consistent with the nano-scale coexistence of regions of  $\alpha$  and  $\beta$  phase in every particle of the (now finer) powder. The much larger degree of elastic accommodation of the

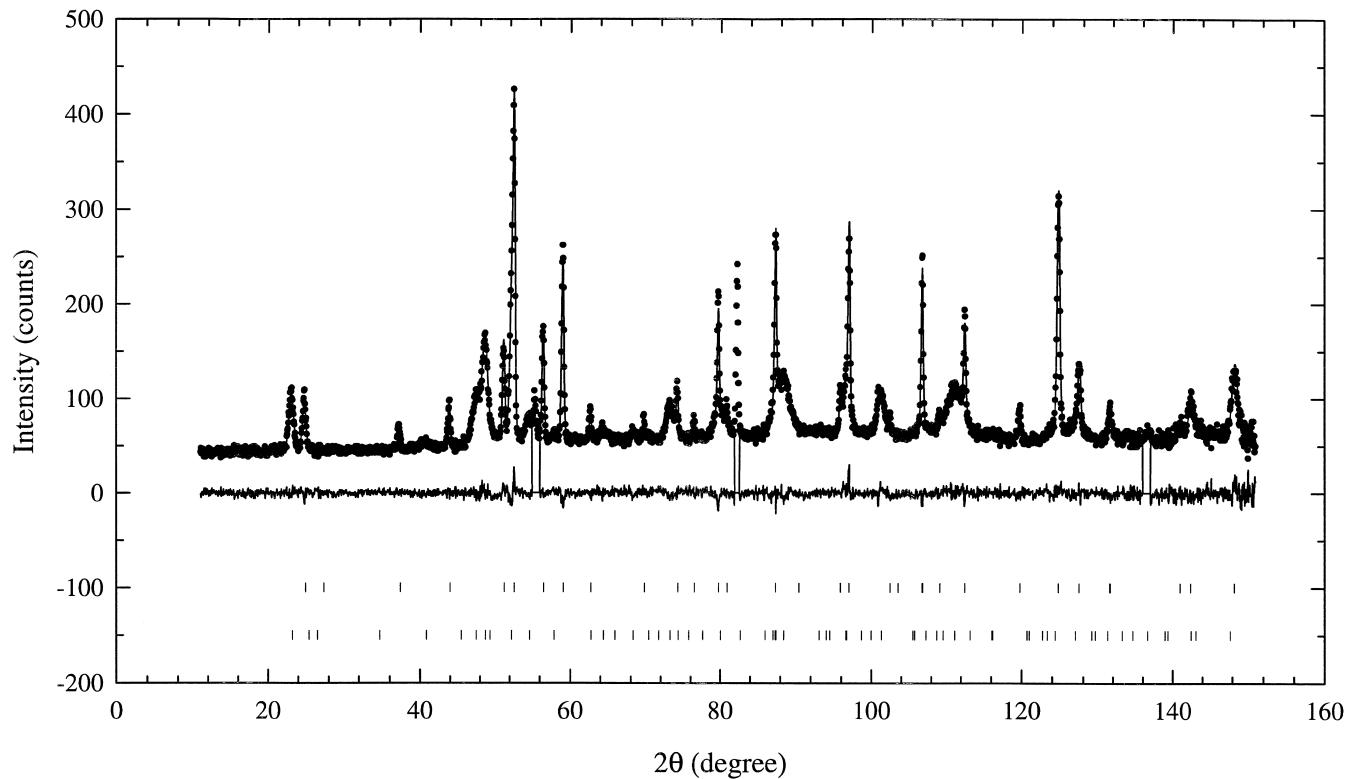


Fig. 2. Typical two-phase diffraction pattern recorded at  $D/M=0.53$  (determined by quantitative phase analysis) in absorption. The measured pattern is indicated by points, the fitted pattern and difference spectrum (below) by lines. The reflection markers are for the  $\alpha$  (upper set) and  $\beta$  (lower set) phases. The excluded regions correspond to the Al pressure chamber. Note the sharpness of the  $\alpha$ -phase peaks, indicating lack of strain, and the characteristic anisotropy of peak breadth in the  $\beta$ -phase peaks.

misfit strain is seen in the dilation of small  $\alpha$ -phase regions present in otherwise  $\beta$ -phase particles near the  $\alpha + \beta/\beta$  phase boundary, and in the compression of  $\beta$ -phase regions present in otherwise  $\alpha$ -phase particles near the  $\alpha/\alpha + \beta$  phase boundary. This is in general agreement with our study of a multiply-cycled sample [12], although the absolute variation in the lattice parameters is rather smaller in the present case, and the non-monotonic variation of  $c_{\beta}$  is not understood. It is barely significant to within  $3\sigma$ .

The absence of resolvable broadening in  $(00l)$  directions is generally consistent with dominant edge dislocations whose Burgers vectors are perpendicular to the  $c$ -axis, among which the  $(a/3) \langle 2\bar{1}10 \rangle \{0\bar{1}10\}$  system best fits the observed diffraction profiles of hydrogen-cycled samples [5,6]. Such dislocations produce no strain (homogeneous or inhomogeneous) in the  $c$  direction. Hence, the substantial expansion of the unit cell in the  $c$  direction between the virgin and cycled states is difficult to explain as a consequence of dislocation generation. A similar result was found in a previous study [2]. One probably important factor is the amount of trapped D. Fig. 4 suggests that  $a_{\alpha}$ , and perhaps  $c_{\alpha}$ , is a sensitive function of D content in the pure-phase region in desorption as well as in absorption: perhaps a more thorough desorption would have decreased both significantly. Another factor is the reality that, while  $(a/3) \langle 2\bar{1}10 \rangle \{0\bar{1}10\}$  is the dominant

dislocation, others have been observed [7] and may cause strain in the  $c$  direction in some circumstances.

The behaviour of the microstrain parameter,  $\Delta a/a$ , is complex, but susceptible to useful qualitative interpretation. During the very first absorption (activation),  $\Delta a/a$  was unresolvable for the  $\alpha$  phase and large for the  $\beta$  phase, exactly as expected if misfit dislocations form at the  $\alpha/\beta$  interface and are left in the wake of the expanding interface prior to fracture. If the  $\beta$ -phase nuclei grew significantly before suffering fracture (with elastic accommodation of the misfit strain, we could expect to see diffraction peaks with a dominantly sharp character. In contrast, the  $\beta$ -phase peaks appear to be wholly broad, demonstrating that each  $\beta$ -phase particle has many dislocations distributed throughout its interior. Furthermore, there is relatively little mechanical damage inflicted on the parent  $\alpha$  phase matrix during the first absorption, in contrast to some published expectations [13]. Hence, the initial  $\alpha$ - $\beta$  transformation is best described as incoherent, in that there is no significant elastic accommodation of the misfit strain. This is a significant issue for understanding the origins of absorption-desorption hysteresis in this system, as coherent and incoherent interfaces have very different thermodynamic consequences [14].

The detailed variation of  $\Delta a/a$  in desorption differs from that observed in an earlier study of a multiply-cycled

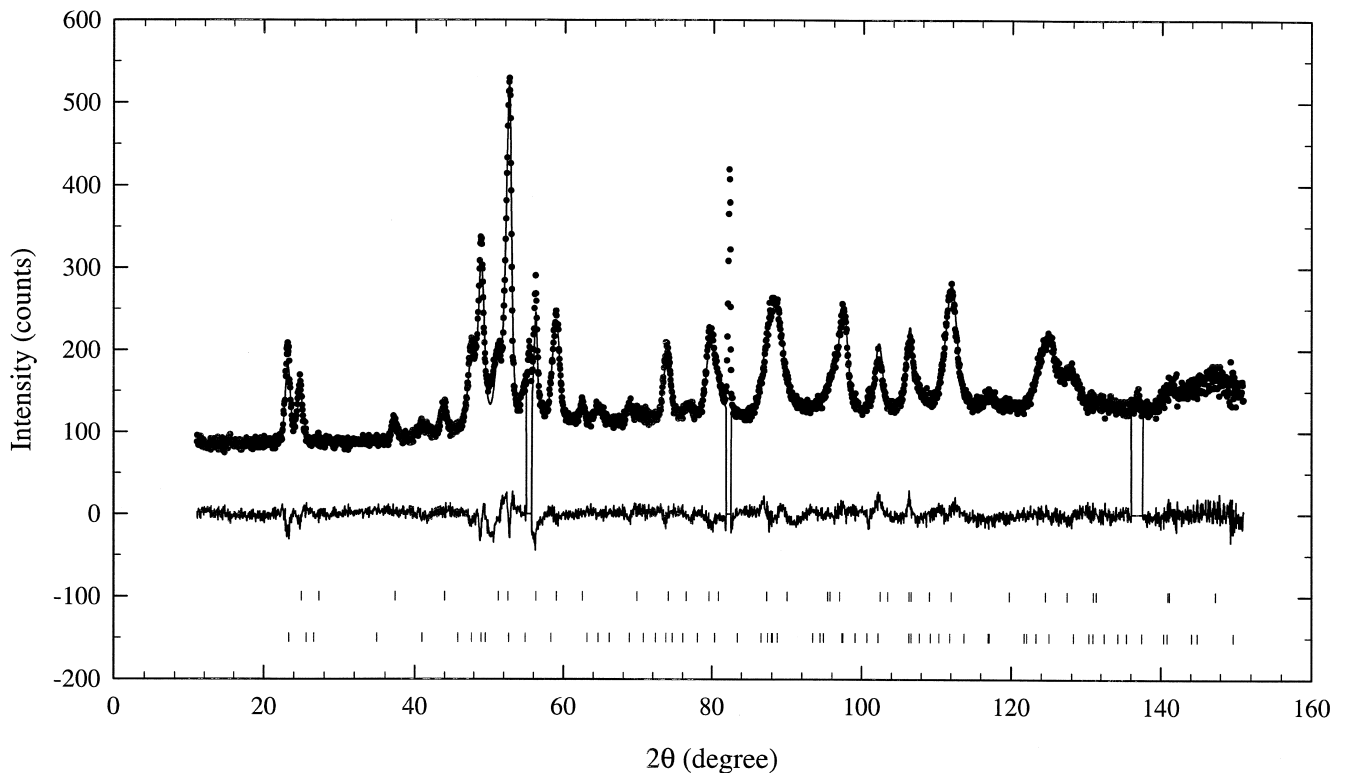


Fig. 3. Typical two-phase diffraction pattern recorded at  $D/M=0.48$  (determined by quantitative phase analysis) in desorption. The measured pattern is indicated by points, the fitted pattern and difference spectrum (below) by lines. The reflection markers are for the  $\alpha$  (upper set) and  $\beta$  (lower set) phases. The excluded regions correspond to the Al pressure chamber. The characteristic anisotropy of peak breadth is now apparent in both phases.

sample [12], although the values lie in a similar range. The latter point demonstrates that the anisotropic broadening is largely established after a single absorption, but the continued changes in the absorption and desorption pressures during the first few absorption–desorption cycles [15] are evidence of an on-going evolution of the microstructure, of which the behaviour of  $\Delta a/a$  may be a symptom.

Generally speaking, homogeneous strain shifts the diffraction peaks and a strain gradient broadens them. In the present case, a strain gradient may arise around dislocations or near the  $\alpha$ – $\beta$  interface, owing to their mechanical interaction, ie, if the interface is partially coherent. Although the  $(hk0)$ -type broadening is fully accounted for by a high density of  $(a/3) \langle 2110 \rangle \{0110\}$  dislocations, a combination of dislocations and inhomogeneous strain in the basal plane owing to other causes cannot be ruled out. The rapid variation of  $a$  for both phases during desorption supports this possibility: within a small island of  $\alpha$  in  $\beta$  (or  $\beta$  in  $\alpha$ ), the coherency strain, which is rather long-ranged, will be relatively homogeneous, and the average or homogeneous component will be high. In contrast, we would expect that in the  $\beta$  (or  $\alpha$ ) matrix containing such a precipitate, the coherency strain would be relatively inhomogeneous, again by virtue of its long range, but that the average strain from this cause would be lower. The data in Figs. 4 and 5 are generally consistent with these

ideas, as long as the  $\alpha$ – $\beta$  interface is essentially incoherent in the  $c$  direction.

The behaviour of  $\Delta a/a$  previously observed in a multi-cycled sample [12] cannot be explained in this way. In that case,  $\Delta a/a$  was greatest for small amounts of  $\alpha$  or  $\beta$  in the other phase, while the average strain was greatest, suggesting greater coherency at the interface. We attempt no further interpretation of this parameter here for the reason that the evolution of the microstructure in the first few cycles deserves a study of its own with data at more values of  $D/M$ .

Finally, we remark on the shortness of the desorption isotherm relative to absorption, equivalent to a loss of recoverable D capacity approaching 0.1 in  $D/M$ . The behaviour of the lattice parameters in the pure  $\alpha$  phase is very similar in absorption and desorption, suggesting that the same process of D ingress/egress to/from the solid solution is occurring, albeit at different values of the total D concentration. Hence a significant fraction of D atoms is trapped. While the manometric measurements of  $D/M$  might be doubted, the effect is very reproducible and trapped H has been directly observed in  $\text{LaNi}_5$  by an independent technique, deep-inelastic neutron scattering [16]. The state of the trapped D is uncertain, although the possibility that dislocation cores act as traps is very plausible given our certainty that dislocations are the dominant crystal defect [6]. The formation of amorphous

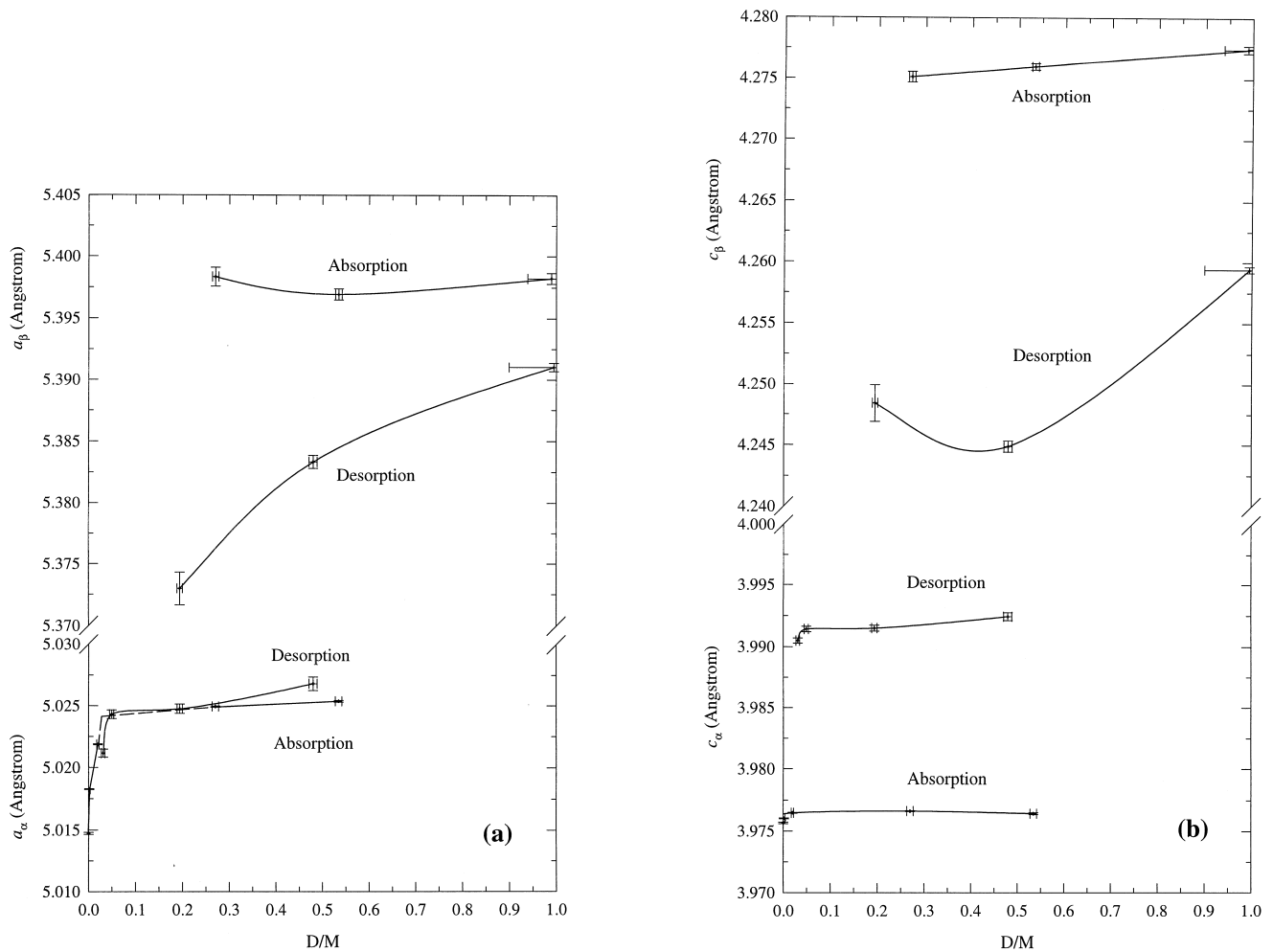


Fig. 4. Unit cell dimensions for  $\alpha$  and  $\beta$  phases (referred to  $P6/mmm$ ), plotted against D/M derived from quantitative phase analysis, as explained in the text. Error bars are  $\pm 1\sigma$ . (a)  $a$ ; (b)  $c$ . Note the general constancy of the lattice parameters in absorption, the effects of partial interface coherence in desorption and the strong dependence of  $a_\alpha$  in particular on D concentration in the pure  $\alpha$  phase.

$\text{LaH}_x$  cannot be entirely ruled out, although no evidence of Ni from such a decomposition of the intermetallic was detected. Neither should binding to the vacancies which exist adjacent to dislocation cores and facilitate their climb [17] be neglected. This issue is further considered elsewhere [18].

## 5. Conclusions

The very first absorption of deuterium by virgin  $\text{LaNi}_5$  occurs by a mechanism which is fundamentally different to that operating in material which has been absorption–desorption cycled:

- the saturation of the  $\alpha$  phase is accompanied by highly anisotropic expansion of the unit cell;
- the  $\beta$  phase physically separates from the parent  $\alpha$  phase and the volume fraction of coexisting  $\alpha$  and  $\beta$  (within the same powder grain) phases is very small;

- the absence of mechanical interaction leads to constant lattice parameters, general compliance with the phase rule, and a flat absorption plateau;
- the  $\beta$  phase contains a high density of lattice defects, apparently dislocations of the type  $(a/3) \langle 2110 \rangle$ , as observed in cycled material, but the  $\alpha$  phase remains relatively undamaged prior to transforming.

During the very first desorption, the microstructure already resembles that observed after many absorption–desorption cycles: the  $\alpha$  and  $\beta$  phases now coexist within the same powder grain, with a significant ability to accommodate interfacial strain coherently, somehow conferred by the dislocations generated during absorption. The microstructure evidently continues to evolve during the first few absorption–desorption cycles.

A significant amount of deuterium, equivalent to almost 0.1 D/M, is trapped in the sample following the first desorption. The trapping appears to be intimately linked to the dislocation generation.

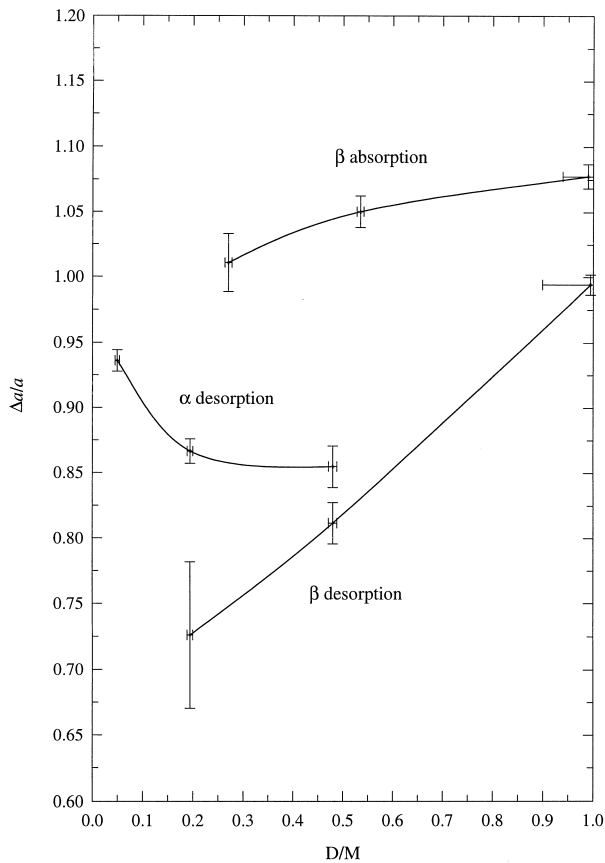


Fig. 5. Variation of the magnitude of anisotropic peak breadth, expressed as generic basal-plane strain. No data are shown for the  $\alpha$  phase in absorption because the broadening was below resolution.  $\Delta a/a$  contains contributions from dislocations (atoms systematically off position) and coherency strain (distributed inter-planar distance).

### Acknowledgements

This work was supported by the Australian Institute of Nuclear Science and Engineering. The help of Dr. Shane Kennedy at ANSTO is also gratefully recognised.

### References

- [1] K. Nomura, H. Uruno, S. Ono, H. Shinozuka, S. Suda, *J. Less-Common Met.* 107 (1985) 221–230.
- [2] E.H. Kisi, C.E. Buckley, E.MacA. Gray, *J. Alloys Comp.* 185 (1992) 369–384.
- [3] P.L. Notten, J.L.C. Daams, A.E.M. de Veirman, A.A. Staals, *J. Alloys Comp.* 209 (1994) 85–91.
- [4] T.B. Flanagan, G.E. Biehl, *J. Less-Common Met.* 82 (1981) 385–389.
- [5] E. Wu, E.MacA. Gray, E.H. Kisi, *J. Appl. Crystallogr.* 31 (1998) 356–362.
- [6] E. Wu, E.H. Kisi, E.MacA. Gray, *J. Appl. Crystallogr.* 31 (1998) 363–368.
- [7] G.H. Kim, S.G. Lee, K.Y. Lee, C.H. Chun, J.Y. Lee, *Acta Metall. Mater.* 43 (1995) 2233–2239.
- [8] E.H. Kisi, E.MacA. Gray, *J. Alloys Comp.* 217 (1995) 112–117.
- [9] R.J. Hill, C. J. Howard, Australian Atomic Energy Commission Rep. AAEC/M 112, Lucas Heights, Australia, 1986.
- [10] C. Lartigue, A. Le Bail, A. Pecheron-Guegan, *J. Less-Common Met.* 129 (1987) 65–76.
- [11] J.L. Soubeyroux, A. Pecheron-Guegan, J.C. Achard, *J. Less-Common Met.* 129 (1987) 181–186.
- [12] E.H. Kisi, E.MacA. Gray, S.J. Kennedy, *J. Alloys Comp.* 216 (1994) 123–129.
- [13] H.K. Birnbaum, *J. Less-Common Met.* 104 (1984) 31–41.
- [14] R.B. Schwarz, A.G. Khachatryan, *Phys. Rev. Lett.* 74 (1995) 2523–2526.
- [15] C.E. Buckley, E.MacA. Gray, E.H. Kisi, *J. Alloys Comp.* 215 (1994) 195–199.
- [16] E.MacA. Gray, M. Kemali, J. Mayers, J. Norland, *J. Alloys Comp.* 253–254 (1997) 291–294.
- [17] R. Griessen, *Phys. Rev. B.* 38 (1988) 3690–3698.
- [18] E.MacA. Gray, T.P. Blach, C.E. Buckley, 293–295 (1999) 57–61.